

## Soil-structure interaction effects on the seismic response of multistory frame structure

Amina Botić<sup>1a</sup>, Emina Hadzalic<sup>\*2</sup> and Anis Balić<sup>2b</sup>

<sup>1</sup>IPSA Institute, Put Života b.b, 71000 Sarajevo, Bosnia and Herzegovina

<sup>2</sup>University of Sarajevo - Faculty of Civil Engineering, Patriotske Lige 30, 71000 Sarajevo, Bosnia and Herzegovina

(Received April 14, 2022, Revised May 4, 2022, Accepted May 20, 2022)

**Abstract.** In this paper, soil-structure interaction effects on the seismic response of multistory frame structure on raft foundation are numerically analyzed. The foundation soil profile is assumed to consist of a clay layer of variable thickness resting on bedrock. A modified plane-strain numerical model is formed in the software Plaxis, and both free vibration analysis, and earthquake analysis for a selected ground motion accelerogram are performed. The behavior of the structure is assumed to be linear elastic with Rayleigh viscous damping included. The behavior of the clay layer is modeled with a Hardening soil model with small strain stiffness. The computed results in terms of fundamental period and structural horizontal displacements for the case of fixed base and for different thicknesses of clay layer are presented, compared, and discussed.

**Keywords:** earthquake; frame; fundamental period; horizontal displacements; response spectrum; seismic load; soil-structure interaction

### 1. Introduction

The design of the structures in seismically active areas must account for the seismic loads that will be exerted on the structure during an expected earthquake. The key parameters that affect the seismic loads are the seismic zone in which the structure is located, the type of the foundation soil, and the dynamic properties of the structure, such as the fundamental period of the structure and damping.

The numerous aspects of seismic analysis of structures are investigated in many research works, such as (El Abbas *et al.* 2016, Løkke and Chopra 2019, Mandal and Maity 2019, Ansari and Jamle 2019, Ademovic *et al.* 2020, Mejia-Nava *et al.* 2021, Gönen and Soyöz 2021) to mention few. The common assumption in the seismic analysis of the structures is that the structure is fixed at the base, thus the effects of the soil-structure interaction are neglected. However, during the earthquake, both the structure and the foundation soil deform, thus mutually affecting their

---

\*Corresponding author, Assistant Professor, E-mail: emina.hadzalic@gf.unsa.ba

<sup>a</sup>Civil Engineer, E-mail: amina.botic@ipsa-institut.com

<sup>b</sup>Assistant Professor, E-mail: anis.balic@gf.unsa.ba

responses. The deformation of the foundation soil leads to the elongation of the fundamental period of the structure and a damping increase. This suggests that the soil-structure interaction affects the response of the structure during the earthquake due to the modified dynamic properties of the structure.

For the structures on stiff soils, the assumption of a fixed base can be considered justified and the effects of the soil-structure interaction can be neglected. On the other hand, for structures on soft soils, the assumption of the fixed base can be too conservative, since the effects of the soil-structure interaction for typical structures with intermediate and long fundamental period usually result in a decrease in the seismic demand, which can lead to the more economical design of the structure. However, the soil-structure interaction can also have a negative effect on the seismic response of the structure, such as in the case of slender structures, structures with pronounced effects of second-order theory, or structures on very soft soils, where the soil-structure interaction can result in a significant increase in the structural displacements (EN 1998-1: Eurocode 8).

The seismic soil-structure interaction was first considered in the structural design of nuclear power plants (Newmark and Hall 1969, Seed and Lysmer 1978). Newmark and Hall (Newmark and Hall 1969), using a relatively small base of earthquake recordings, showed that cross-section forces decrease when compared to the structure on the bedrock and that for softer soils damping increase is expected. The soil-structure interaction effects on the seismic response of moment-resisting frames, a structural system frequently encountered in everyday engineering practice that carries both vertical and horizontal load, is the subject of many research works. Jennings and Bielak (1973) analyzed the dynamics of building-soil interaction by modeling the soil by a linear elastic half-space and the building structure by an  $n$ -degree-of-freedom oscillator. In their research, they concluded that the influence of soil-structure interaction is predominantly related to the fundamental mode for many  $n$ -story structures and that this influence can be neglected for higher modes, especially for tall buildings. They also concluded that the fundamental period for softer soils generally increases. Galal and Naimi (2008) based on the results of a detailed numerical analysis of a 6-story and 20-story reinforced concrete frame structure, in which the soil is modeled with springs, concluded that the effects of soil-structure interaction become significant when the shear wave velocity  $v_s$  is less than 600 m/s. Similar conclusions are reported in (Tabatabaiefar *et al.* 2013). Tabatabaiefar and Massumi (2010) reported that it is essential to consider the effects of soil-structure interaction for reinforced concrete frames higher than three stories resting on the soil with  $v_s$  less than 175 m/s, and for frames higher than seven stories resting on the soil with  $v_s$  ranging from 175 m/s to 375 m/s. Raheem *et al.* (2014) performed a numerical finite element method analysis of the response of a multistory frame structure on a raft foundation, in which the foundation soil is modeled with Winkler springs. They concluded that the soil-structure interaction results in an elongation of the fundamental period, and an increase in lateral displacements, especially for softer soils. Lu *et al.* (2016) conducted a comprehensive parametric study of multistory shear buildings by using a discrete-element model for simulating the dynamic behavior of foundation resting on soil, and they outlined that soil-structure interaction can reduce (up to 60%) the strength and ductility demands of multistory buildings, especially those with small slenderness ratio and low ductility demands. Kabtamu *et al.* (2018) using Winkler springs and half space direct method models studied the response of 7-story and 12-story reinforced concrete frames on soft soils subjected to ground motion, and reported that soil-structure interaction results in a bigger fundamental period and inter story drift but smaller base shear than fixed base case. Zhang and Far (2021) performed a numerical finite element analysis of 20, 30 and 40-story building on soft soil subjected to earthquake. They concluded, among others, that the soil-structure

interaction can increase the maximum lateral displacement of the structure, but for high-rise structures, an increase in height does not necessarily imply an increase in the maximum lateral displacements, because of the elongation of the fundamental period combined with the ground motion features. Aside the common assumption of a linear elastic behavior, various research works aim to model the nonlinearities in the soil, structure, or both due to the damage and fracture that occurs during the loading, which can modify the dynamic response, such as (Brancherie and Ibrahimbegovic 2009, Do and Ibrahimbegovic 2018, Hadzalic *et al.* 2018a, Hadzalic *et al.* 2018b, Nikolić *et al.* 2018) to mention few.

In this paper, soil-structure interaction effects on the seismic response of the multistory reinforced concrete moment-resisting frame structure on a raft foundation are numerically investigated. The foundation soil profile is assumed to consist of a clay layer of variable thickness resting on bedrock. A modified plane-strain finite element numerical model of soil-structure interaction is formed in the software Plaxis. The behavior of the structure is assumed to be linear elastic with Rayleigh viscous damping included. The behavior of the clay layer is modeled with a Hardening soil model with small strain stiffness. Both free vibration analysis and earthquake analysis are performed. The aim is to examine how the thickness of the soft clay layer through the soil-structure interaction affects the fundamental period of the frame structure of interest and subsequently the response of the frame structure subjected to earthquake, in terms of structural displacements and forces.

The outline of the paper is as follows. In Section 2, we describe the main details of the numerical model of soil-structure interaction formed in the software Plaxis. In Section 3, we present and discuss the computed results. In Section 4, we give our concluding remarks.

## 2. Numerical model

The numerical model of soil-structure interaction is formed in the software Plaxis. The main details of the model concerning model geometry, parameters of model elements, and performed analyses are presented next.

### 2.1 Model geometry

The geometry of the multistory frame structure resting on a raft foundation is shown in Fig. 1. The frame structure has six floors, each 3 m high, resulting in a total height of 18 m. The disposition of the frame structure is regular with frames equally separated by  $l_a=5$  m, resulting in the total dimensions of the structure of 10×20 m. To model the response of the 3D multistory frame structure, a modified plane-strain approach is utilized (Robert 2009). Namely, if the dimension of the raft foundation is significantly larger in one direction ( $y$ - direction), then it can be assumed that the raft foundation is infinitely rigid for bending in the plane containing that direction. This allows us to model the 3D multistory frame structure with an equivalent plane-strain model for a shorter  $x$ - direction, while the contribution of the transverse elements to the stiffness can be neglected. To adequately take into account the soil-structure interaction, the dimension of the model in  $y$ - direction has to be equal to the  $l_a$  (Robert 2009), which in this case is 5 m.

The dimension of the numerical model in  $x$ - direction (model width) of 200 m is chosen to eliminate the influence of boundary conditions. The thickness of the clay layer varies from 2 m to

10 m, thus the depth of the model varies accordingly from 3 m to 11 m, where an additional 1 m is the thickness of the bedrock, which remains constant in all numerical simulations. The numerical model of soil-structure interaction is shown in Fig. 2.

The soil response is approximated with 10-node tetrahedral finite element, the raft foundation response with 6-node triangular Mindlin plate finite element and the response of the beams and columns with 3-node Mindlin beam finite element. For details of the selected finite element approximations, see (Plaxis Scientific Manual 2021). The presence of groundwater is not analyzed in this study.

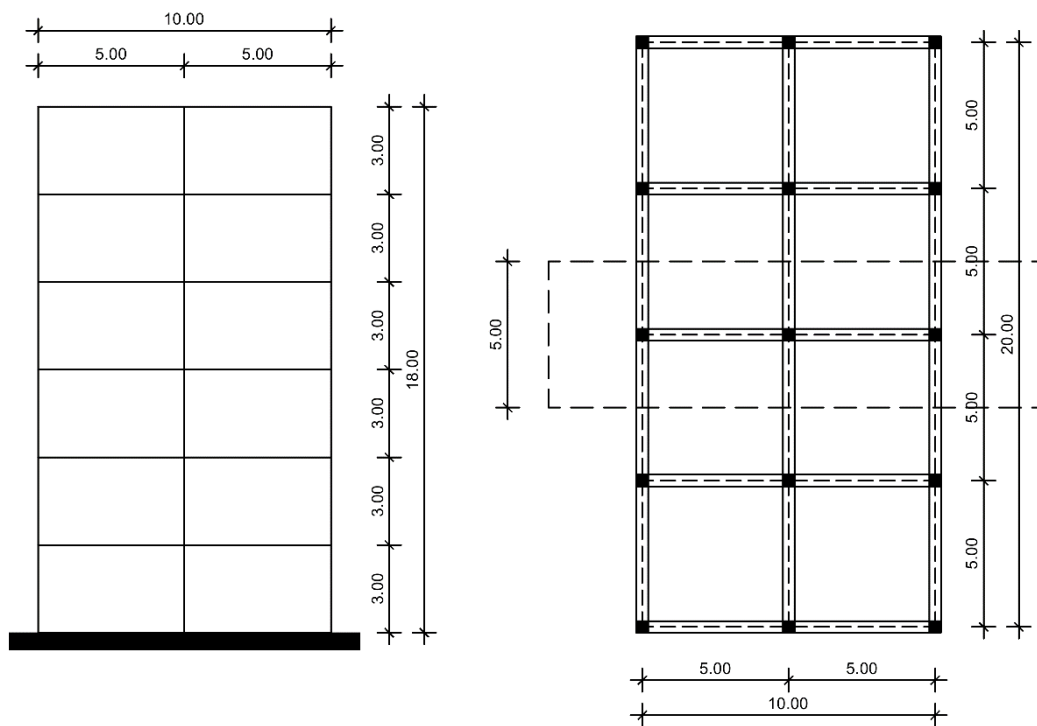


Fig. 1 Geometry of the multistory frame structure

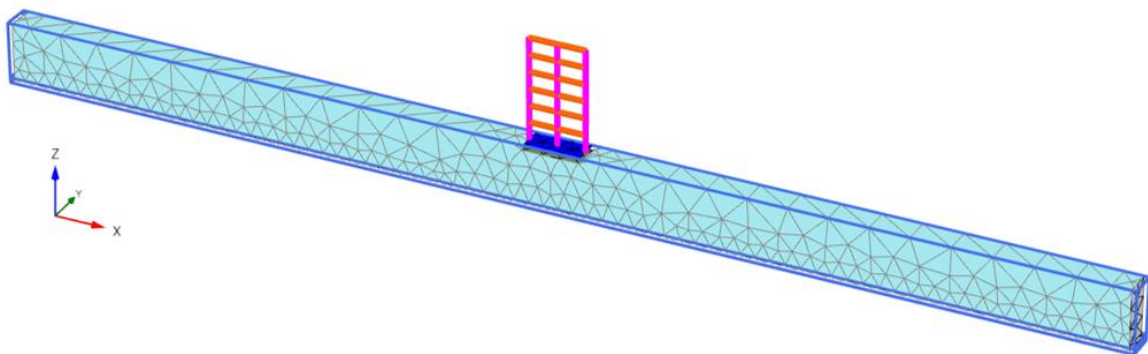


Fig. 2 Numerical model of soil-structure interaction

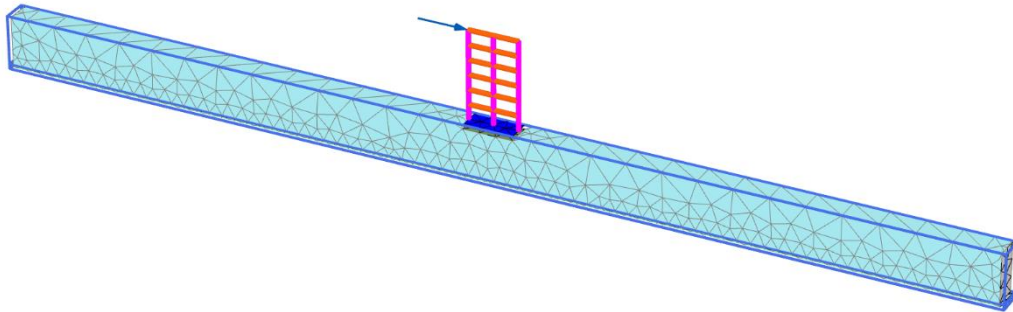


Fig. 3 Horizontal force imposed on the frame

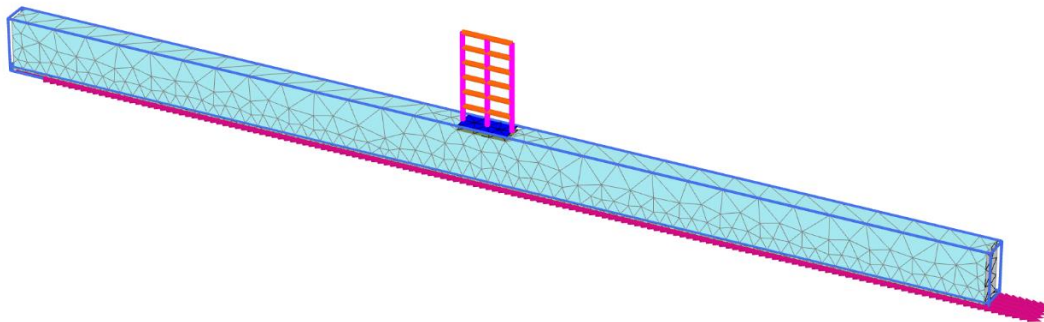


Fig. 4 Uniform line displacements in  $x$ - direction imposed on the bottom model boundary

### 2.3 Types of analysis

To investigate soil-structure interaction effects, both free vibration analysis and earthquake analysis are performed. Both analyses have in common the first two calculation phases.

The first phase is the  $K_0$  procedure, in which the initial stress, strain, and displacement fields in the soil are computed. In the second phase, the structure, i.e., the frame is constructed and the stress, strain, and displacement fields due to structural loads are evaluated. The structural loads include self-weight of the structural elements and additional self-weight of floors, computed by taking into account the tributary area. The additional self-weight of the floor is assumed to be 5 kN/m<sup>2</sup>. The first two calculation phases are plastic types of calculation, in which the elastic-plastic deformation analysis is performed. The boundary conditions for plastic calculation consists of prevented displacements in  $x$ - direction for vertical model boundaries with their normal in  $x$ -direction (lateral boundary), prevented displacements in  $y$ - direction for vertical model boundaries with their normal in  $y$ - direction, and prevented displacements in all directions on the bottom model boundary.

The free vibration analysis includes two additional phases. Namely, in the third phase, the horizontal force of 100 kN at the upper left corner of the frame is applied and plastic calculation is again performed (Fig. 3). In the fourth phase, the action of the force is removed and the frame is allowed to vibrate freely. The total duration of this phase, which is a dynamic type of calculation, is 5 sec. To perform free vibration analysis, additional, viscous boundary conditions are imposed on the bottom and lateral boundaries of the model (Plaxis Reference Manual 2021).

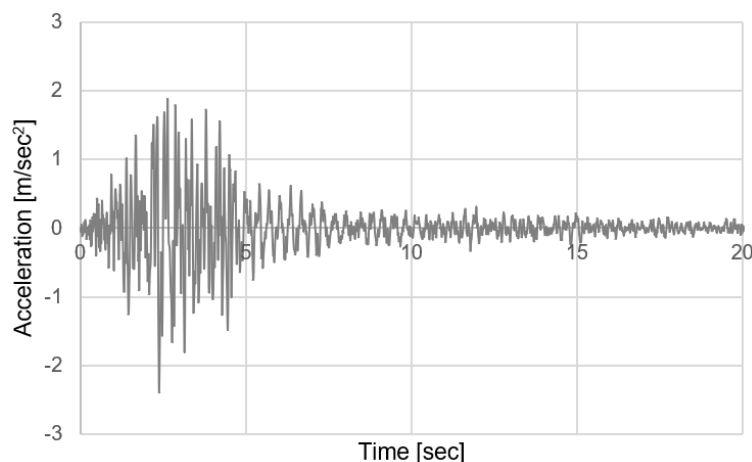


Fig. 5 Accelerogram of ground motion for the Upland earthquake (1990)

The earthquake analysis includes one additional dynamic phase, in which the frame is subjected to an earthquake. The earthquake is modeled by introducing the compliant base boundary conditions and a uniform line displacement in  $x$ - direction at the bottom model boundary (Fig. 4). The displacement in  $x$ - direction is multiplied by the corresponding dynamic multiplier obtained from the ground motion accelerogram (Plaxis Reference Manual 2021). The displacements in  $y$ - and  $z$ - directions are prevented. The free-field boundary conditions are imposed on the lateral boundaries of the model (Plaxis Reference Manual 2021), with the displacements in  $x$ - direction remaining prevented. In all numerical simulations, the ground motion accelerogram for the Upland earthquake (1990) is used (Fig. 5). The input motion duration is 20 sec with time intervals of 0.005 sec.

The unknown nodal displacements, velocities, and accelerations, are computed on the global level by solving the second-order differential equations of motion in time; for linear elastic system written as

$$\mathbf{M}\ddot{\mathbf{u}} + \mathbf{C}\dot{\mathbf{u}} + \mathbf{K}\mathbf{u} = \mathbf{F} \quad (1)$$

where  $\mathbf{M}$  is the mass matrix,  $\mathbf{C}$  is the damping matrix,  $\mathbf{K}$  is the stiffness matrix,  $\mathbf{F}$  is the load vector,  $\mathbf{u}$  is the vector of unknown nodal displacements,  $\dot{\mathbf{u}}$  is the vector of unknown nodal velocities, and  $\ddot{\mathbf{u}}$  is the vector of unknown nodal accelerations. The resulting matrices and vectors are obtained by performing a standard finite element discretization procedure. The damping matrix is obtained by assuming Rayleigh viscous damping, written as

$$\mathbf{C} = \alpha_R \mathbf{M} + \beta_R \mathbf{K} \quad (2)$$

where  $\alpha_R$  and  $\beta_R$  are Rayleigh damping coefficients.

To solve the second-order differential equations of motion, the implicit time integration scheme of Newmark is utilized, where the unknown nodal displacements and velocities are approximated in the following manner

$$u^{t+\Delta t} = u^t + \dot{u}^t \Delta t + \left( \left( \frac{1}{2} - \alpha_N \right) \ddot{u}^t + \alpha_N \ddot{u}^{t+\Delta t} \right) \Delta t^2$$

$$\dot{u}^{t+\Delta t} = \dot{u}^t + \left( (1 - \beta_N)\ddot{u}^t + \beta_N\ddot{u}^{t+\Delta t} \right) \Delta t \quad (3)$$

where,  $\Delta t$  is the time step, and  $\alpha_N, \beta_N$  are Newmark coefficients, which determine the accuracy of the time integration scheme. The recommended values of Newmark coefficients are  $\alpha_N=0.25$ , and  $\beta_N=0.5$ , which yield an average acceleration method (Plaxis Scientific Manual 2021).

If the behavior of the model elements, whether it is structural elements or soil, is assumed nonlinear, the incremental-iterative procedure has to be employed. Here, at each time step, the tangent stiffness matrix is formed, which depends on the constitutive model selected for a specific model element. Due to the change in the tangent stiffness matrix, the Rayleigh damping is not recommended to use to model the viscous damping of a model element with nonlinear behavior.

#### 2.4 Geometric and material properties of model elements

The raft foundation is 0.6 m thick. The cross-section dimensions of the beams are 0.4x0.5 m, and the cross-section dimensions of the columns are 0.5x0.5 m. The behavior of all structural elements is assumed to be linear elastic, with Young's modulus of concrete  $E=3 \cdot 10^7$  kN/m<sup>2</sup>. The Rayleigh damping parameters are  $\alpha_R=0.2$  and  $\beta_R=0.008$ . The behavior of bedrock is linear elastic, with a large value of Young's modulus  $E=10^{21}$  kN/m<sup>2</sup> selected to model hard rock.

The behavior of the clay is modeled with a Hardening soil model with small-strain stiffness (Benz 2006), which is an extension of the frequently used Hardening soil model (Schanz and Vermeer 1998, Schanz *et al.* 1999). The Hardening soil model (HS) is a plasticity type of model, which assumes that plastic strains in soil occur immediately when the deviatoric loading is applied. The main features of the HS model are the hyperbolic relationship between the vertical strain and deviatoric stress; the stress dependent stiffness defined with a power law; elastic unloading/reloading stiffness; failure according to the Mohr-Coulomb failure criterion. Two types of hardening mechanisms are implemented in the model. The shear hardening models the plastic strains developed due to deviatoric loading, and the cap hardening models the plastic strains due to primary compression.

The HSsmall model is an enhanced version of the HS model with additional features pertaining to the very small-strain soil stiffness and its nonlinear dependency on the strain (Fig. 6) defined with a modified Hardin-Drnevich relationship (Hardin and Drnevich 1972, Santos and Correia 2001). The variation of the stiffness with strain is defined as follows

$$G_s = \frac{G_0}{\left(1 + 0.385 \frac{\gamma}{\gamma_{0.7}}\right)^2} \quad (4)$$

where  $G_0$  is the small-strain shear modulus,  $G_s$  is the secant shear modulus,  $\gamma$  is the shear strain and  $\gamma_{0.7}$  is the shear strain at which the secant shear modulus is  $G_s=0.722G_0$ .

The parameters of the HSsmall model of the clay layer are shown in Table 1. The value of reference shear modulus at very small strain  $G_0^{ref}$  is selected based on the unit mass of the clay  $\rho$  and assumed shear wave velocity in clay layer  $v_s=150$  m/s through the following expression

$$G_0^{ref} = \rho v_s^2 \quad (5)$$

The HSsmall model shows a hysteretic behavior in cyclic loading, which leads to damping. The amount of hysteretic damping depends on the value of applied load and corresponding strain

Table 1 The HSsmall parameters of the clay layer

Parameter	Symbol	Unit	Value
Unit weight	$\gamma_{sat}$	kN/m <sup>3</sup>	20
Secant stiffness in standard drained triaxial test	$E_{50}^{ref}$	kN/m <sup>2</sup>	$2 \cdot 10^3$
Tangent stiffness for primary oedometer loading	$E_{oed}^{ref}$	kN/m <sup>2</sup>	$2 \cdot 10^3$
Unloading/reloading stiffness from drained triaxial test	$E_{ur}^{ref}$	kN/m <sup>2</sup>	$6 \cdot 10^3$
Power for stress-level dependency of stiffness	$m$	-	0.5
Poisson's ratio for unloading-reloading	$\nu_{ur}$	-	0.2
Reference shear modulus at very small strains ( $\epsilon < 10^{-6}$ )	$G_0^{ref}$	kN/m <sup>2</sup>	$46 \cdot 10^3$
Threshold shear strain at which $G_s = 0.722G_0$	$\gamma_{0.7}$	-	$1 \cdot 10^{-3}$
Cohesion	$c$	kN/m <sup>2</sup>	15
Friction angle	$\varphi$	degrees [°]	20
Dilatancy angle	$\psi$	degrees [°]	0
Coefficient of earth pressure at rest	$K_0$	-	0.658

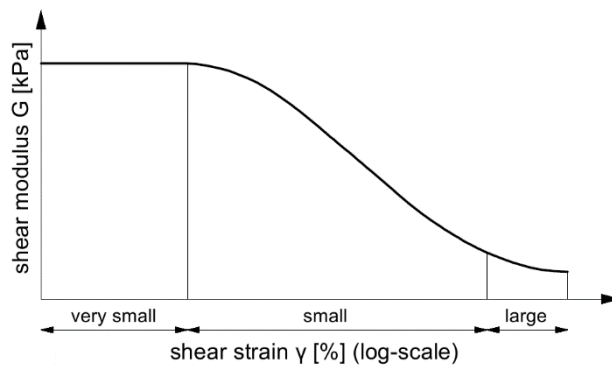


Fig. 6 Shear stiffness variation (Atkinson and Sallfors 1991)

amplitude (Plaxis Material Models Manual 2021). This feature combined with the very small-strain stiffness makes this model convenient to use in dynamic analysis, such as the earthquake analysis.

### 3. Numerical results

#### 3.1 Free vibration analysis

To investigate the influence of soil-structure interaction on the fundamental period of the frame, the free vibration analysis is performed first for the case of the fixed base. Here, the soil domain is deactivated and the displacement of the raft foundation in all directions is prevented. The deformed configuration of the frame with a fixed base is shown in Fig. 7. The computed free vibrations of the frame at point A (-5; 2.5; 18) are shown in Fig. 8. The fundamental period value of 0.876 is read in Fig. 8. This fundamental period corresponds to the case of damped vibrations.



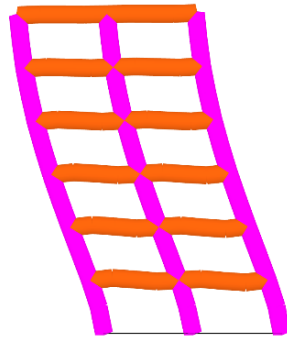


Fig. 7 Deformed configuration of the frame with a fixed base

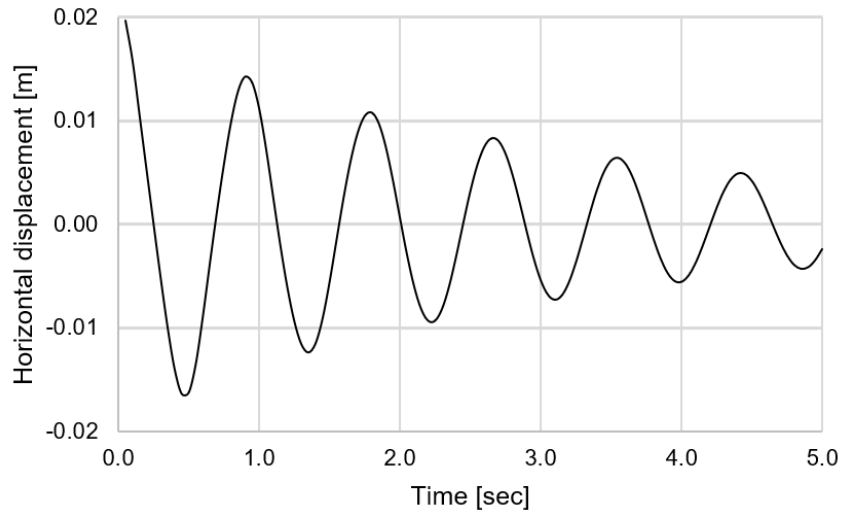


Fig. 8 Free vibrations of the frame with a fixed base

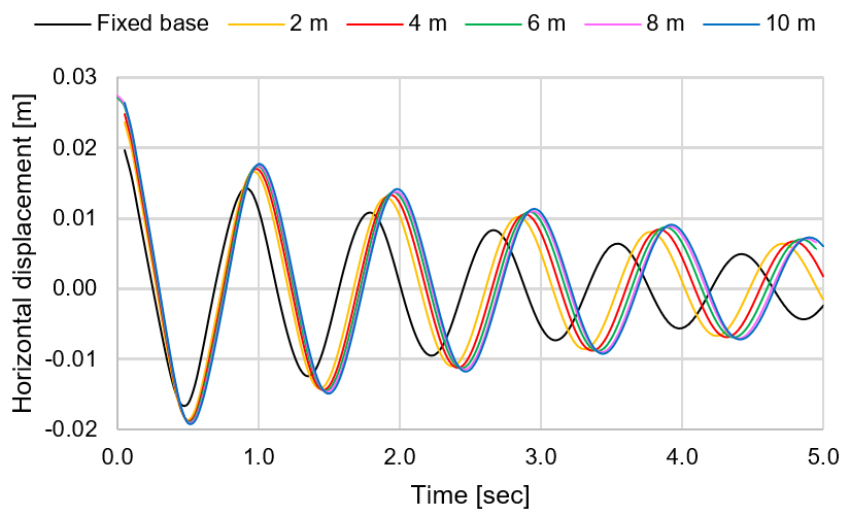


Fig. 9 Free vibrations of the frame for different thicknesses of the clay layer

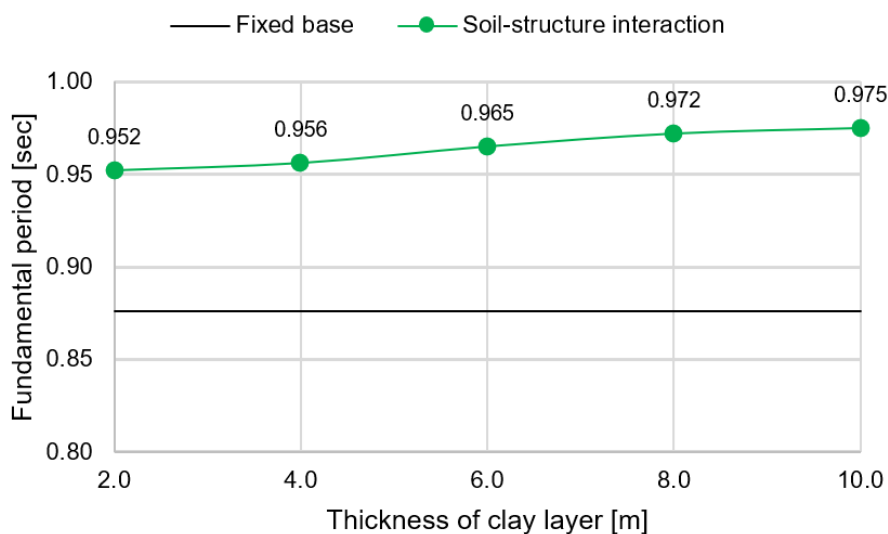


Fig. 10 Comparison of fundamental periods of the frame with respect to the case of a fixed base

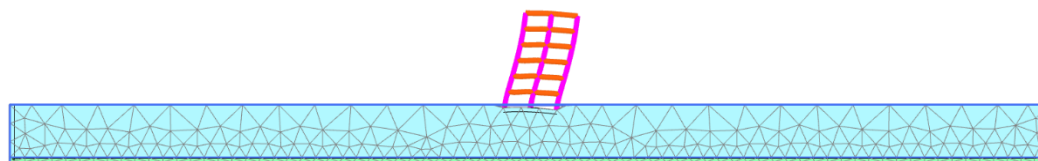


Fig. 11 Deformed configuration of the frame for the 10 m thick clay layer

Next, the free vibration analysis is performed for different thicknesses of the clay layer. The computed free vibrations of the frame at point A (-5; 2.5; 18) are shown in Fig. 9. It can be concluded that the soil-structure interaction results in an elongation of the fundamental period of the frame. This elongation is greater the thicker the clay layer is. Namely, the fundamental period is inversely proportional to the stiffness. Hence, the thicker the clay layer is, the frame becomes more flexible, resulting in a longer fundamental period. The comparison of fundamental periods with respect to the case of the fixed base is shown in Figs. 10. The elongation of the fundamental period for the 2 m thick clay layer is 8.68%, and for the 10 m thick layer 11.30%. The deformed configuration of the frame, for the 10 m thick clay layer, is shown in Fig. 11.

Based on the computed results in terms of the fundamental period, and by appealing to the equivalent static analysis, one of the frequently used methods of seismic analysis in the seismic design, a remark regarding the seismic force exerted on the frame during an expected earthquake can be drawn. Namely, the equivalent static analysis takes into account the effects of an expected earthquake through the static force distributed laterally. This method assumes that the structure dominantly responds in its fundamental lateral mode, and thus the static force is distributed accordingly. The input parameters that determine the value of the equivalent static lateral force are the mass of the structure, the seismic zone in which the structure is located, the local ground conditions, and the dynamic properties of the structure through the fundamental period of the structure and damping.

The input parameters that determine the value of the equivalent static lateral force are the mass

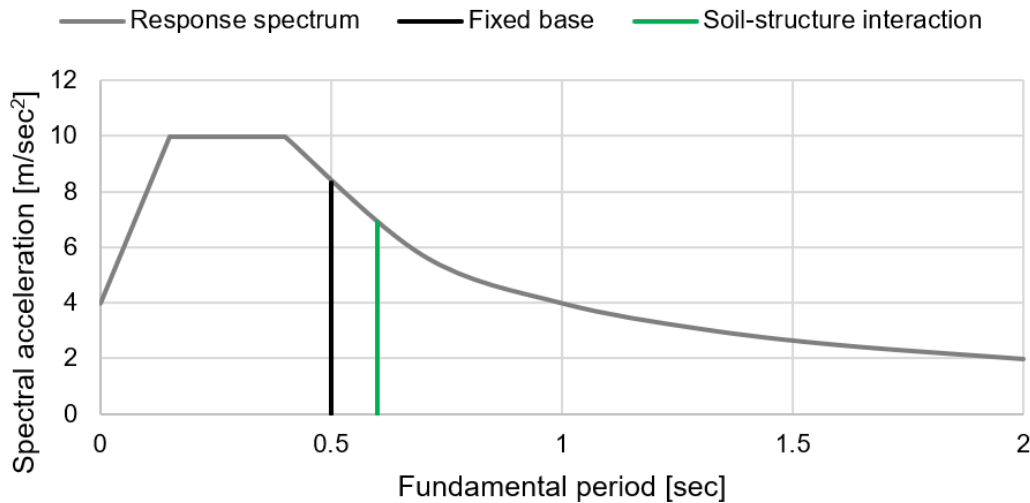


Fig. 12 Illustration of influence of elongation of the fundamental period on the ordinate of the typical acceleration response spectrum

of the structure and the ordinate of the acceleration response spectrum at the fundamental period of the structure for the lateral motion in the direction considered. The response spectrum is one of the basic representations of the seismic action, aside from time history representation. In general, the ground motion response spectrum represents an envelope of the peak responses (displacement, velocity, or acceleration) of multiple single-degree-of-freedom systems with different fundamental periods. The acceleration response spectrum to be used in the seismic analysis of the structures, proposed in EN 1998-1: Eurocode 8, takes into account the seismicity of the area and the local ground conditions. If the behavior of the structure is assumed to remain linear elastic during an expected earthquake, for determining the static lateral force an elastic acceleration response spectrum is used. If the ability of the structure to dissipate energy through nonlinear behavior is taken into account, then static lateral force is computed based on the design acceleration response spectrum. In each case, the same statement can be drawn. Namely, by observing Fig. 12, it can be concluded that for structures with an intermediate or long fundamental period, the elongation of the fundamental period results in a decreased value of the ordinate of the acceleration response spectrum, hence resulting in a decreased value of static lateral force exerted on the structure during an expected earthquake.

### 3.2 Earthquake analysis

To investigate the influence of soil-structure interaction on the structural displacements, a dynamic analysis of the frame subjected to a ground motion is performed. The computed results in terms of horizontal displacements at point A (-5; 2.5; 18) for different thicknesses of clay layer and for ground motion accelerogram for the Upland earthquake are shown in Fig. 13. The comparison of maximum horizontal displacement of the frame at point A for different thicknesses of clay layer against that obtained for the case of a fixed base is shown in Fig. 14. It can be concluded that soil-structure interaction results in an increase in the value of computed horizontal displacements. The maximum horizontal displacement of the frame for the case of a fixed base is 0.036 m. The

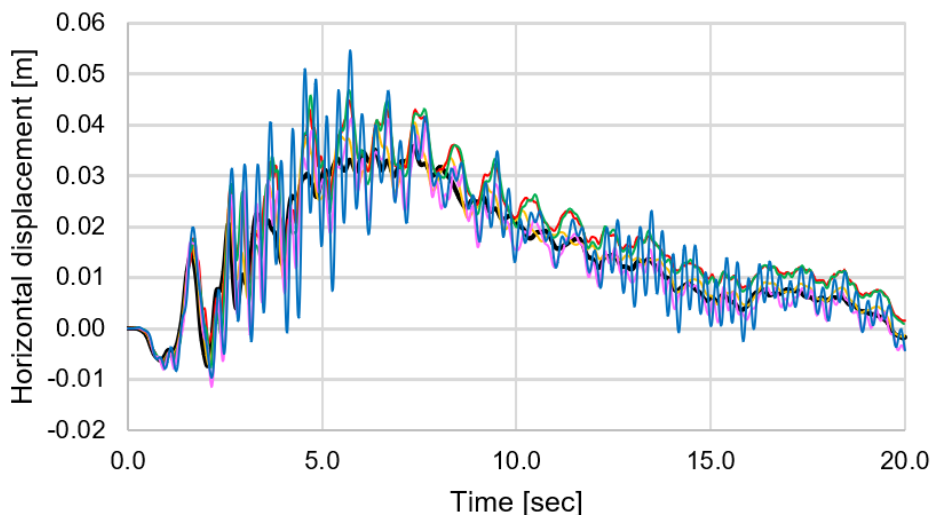


Fig. 13 Horizontal displacements of the frame for different thicknesses of the clay layer

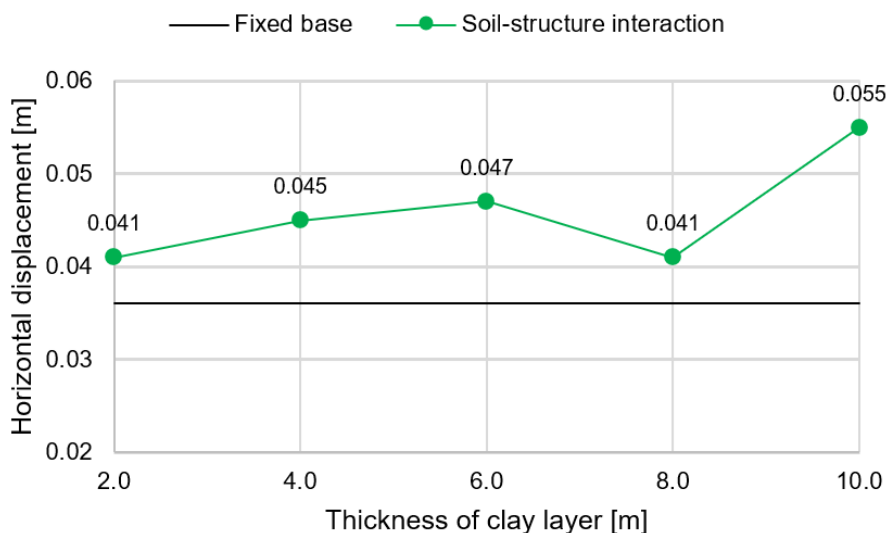


Fig. 14 Comparison of horizontal displacements of the frame with respect to the case of a fixed base

maximum horizontal displacement of the frame for the 2 m thick clay layer is 0.041 m, which is an increase of 13.89%, and for the 10 m thick clay layer 0.055 m, which is an increase of 52.78%.

The results shown in Fig. 14 suggest that the maximum horizontal displacement of the frame tends to increase with an increase in the thickness of the clay layer. However, a deviation in the monotonic trend is observed for the case of the 8 m thick clay layer. To investigate this further, additional computations for thicknesses of clay layer up to 20 m are performed. The computed results are shown in Fig. 15. It can be concluded that the maximum horizontal displacement does not necessarily increase with an increase in the thickness of the clay layer, due to the dynamic factors related to the problem, which, in this case, concern the selected ground motion features and

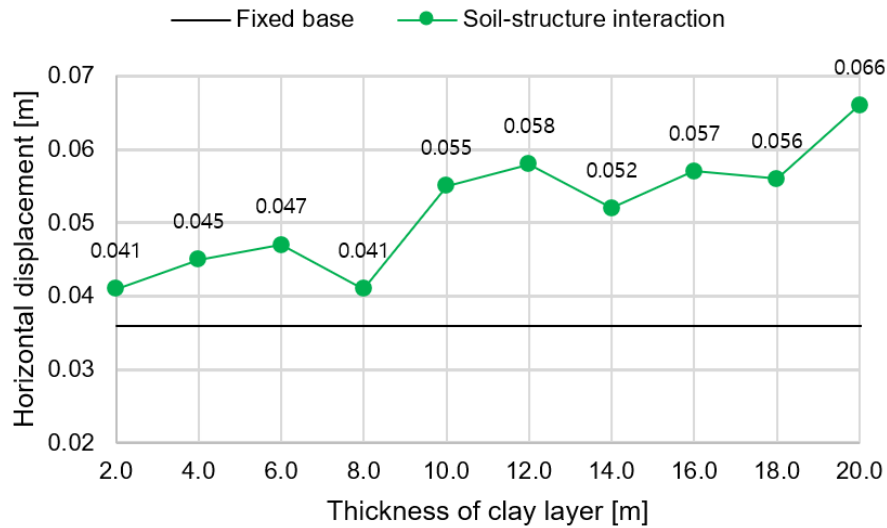


Fig. 15 Comparison of horizontal displacements of the frame with respect to the case of a fixed base, additional computations

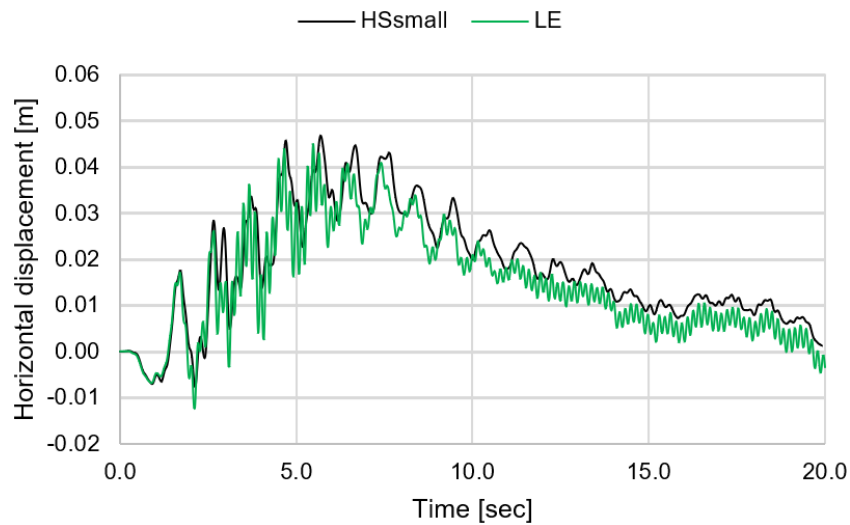


Fig. 16 Comparison of horizontal displacements of the frame for the 6 m thick clay layer, different constitutive models

depth/material properties of the clay layer. A comparable observation is reported in (Zhang and Far 2021) as previously mentioned in the introductory part.

To investigate the influence of the selected constitutive model for the clay on the computed results, an earthquake analysis is also performed for linear elastic behavior with no Rayleigh viscous damping, for the case of the 6 m thick clay layer. The shear modulus of clay layer  $G$  in a linear elastic model is equal to the reference shear modulus at a very small strain  $G_0^{ref}$  in the HSsmall model. The computed horizontal displacements at point A (-5; 2.5; 18) are shown in Fig. 14. The computed horizontal displacements are more smoothed for the case of the HSsmall model

due to hysteretic damping. Also, the use of the HSsmall model results in an increase in the horizontal displacements, due to the loss in stiffness with increasing strain implemented in the model.

## 5. Conclusions

In this paper, the seismic response of multistory frame structure on raft foundation is numerically analyzed. Both free vibration analysis, and earthquake analysis for a selected ground motion accelerogram are performed, with an aim to examine the influence of the clay layer thickness on the seismic response of the structure. Based on the results obtained from free vibration analysis, it is concluded that the soil-structure interaction results in an elongation of the fundamental period of the structure, subsequently resulting in a decrease in the seismic demand, for structures with intermediate or long fundamental periods. The elongation of the fundamental period is greater, the thicker the clay layer is. Moreover, following the results of the earthquake analysis, the soil-structure interaction leads to an increase in the structural horizontal displacements compared to the fixed base case. However, the increase in the horizontal displacements does not necessarily follow an increase in the thickness of the clay layer in a monotonic trend, due to the dynamic factors influencing the problem.

## References

- Abdel Raheem, S.E., Ahmed, M.M. and Alazrak, T. (2014), "Soil-structure interaction effects on seismic response of multi-story buildings on raft foundation", *J. Eng. Sci.*, **42**(4), 905-930.
- Ademović, N., Hadzima-Nyarko, M. and Zagora, N. (2020), "Seismic vulnerability assessment of masonry buildings in Banja Luka and Sarajevo (Bosnia and Herzegovina) using the macroseismic model", *Bull. Earthq. Eng.*, **18**(8), 3897-3933. <https://doi.org/10.1007/s10518-020-00846-8>.
- Ansari, T.A. and Jamle, S. (2019), "Performance based seismic analysis of regular RC building", *Int. J. Manage. Technol. Eng.*, 342-351.
- Atkinson, J.H. and Salfors, G. (1991), "Experimental determination of soil properties", *Proceedings of the 10th ECSMFE*, **3**, 915-956.
- Benz, T. (2006), "Small-strain stiffness of soils and its numerical consequences", Ph.D. Thesis, Universität Stuttgart.
- Brancherie, D. and Ibrahimbegovic, A. (2009), "Novel anisotropic continuum-discrete damage model capable of representing localized failure of massive structures: Part I: Theoretical formulation and numerical implementation", *Eng. Comput.*, **26**(1/2), 100-127. <https://doi.org/10.1108/02644400910924825>.
- Do, X. and Ibrahimbegovic, A. (2018), "2D continuum viscodamage-embedded discontinuity model with second order mid-point scheme", *Couple. Syst. Mech.*, **7**, 669-690. <https://doi.org/10.12989/csm.2018.7.6.669>.
- El Abbas, N., Khamlichi, A. and Bezzazi, M. (2016), "Seismic response of foundation-mat structure subjected to local uplift", *Couple. Syst. Mech.*, **5**(4), 285-304. <https://doi.org/10.12989/csm.2016.5.4.285>.
- EN 1998-1: Eurocode 8 (2004), Design of Structures for Earthquake Resistance-Part 1: General Rules, Seismic Actions and Rules for Buildings, European Committee for Standardization.
- Galal, K. and Naimi, M. (2008), "Effect of soil conditions on the response of reinforced concrete tall structures to near-fault earthquakes", *Struct. Des. Tall Spec. Build.*, **17**(3), 541-562. <https://doi.org/10.1002/tal.365>.
- Gönen, S. and Soyöz, S. (2021), "Seismic analysis of a masonry arch bridge using multiple methodologies", *Eng. Struct.*, **226**, 111354. <https://doi.org/10.1016/j.engstruct.2020.111354>.

- Hadzalic, E., Ibrahimbegovic, A. and Dolarevic, S. (2018), "Failure mechanisms in coupled soil-foundation systems", *Couple. Syst. Mech.*, **7**, 27-42. <https://doi.org/10.12989/csm.2018.7.1.027>.
- Hadzalic, E., Ibrahimbegovic, A. and Nikolic, M. (2018), "Failure mechanisms in coupled poro-plastic medium", *Couple. Syst. Mech.*, **7**, 43-59. <https://doi.org/10.12989/csm.2018.7.1.043>.
- Hardin, B.O. and Drnevich, V.P. (1972), "Shear modulus and damping in soils: Design equations and curves", *Proc. ASCE: Journal of the Soil Mechanics and Foundations Division*, **98**(SM7), 667-692.
- Jennings, P.C. and Bielak, J. (1973), "Dynamics of building-soil interaction", *Bull. Seismol. Soc. Am.*, **63**(1), 9-48. <https://doi.org/10.1785/BSSA0630010009>.
- Kabtam, H.G., Peng, G. and Chen, D. (2018), "Dynamic analysis of soil structure interaction effect on multi story RC frame", *Open J. Civil Eng.*, **8**, 426-446. <https://doi.org/10.4236/ojce.2018.84030>.
- Løkke, A. and Chopra, A.K. (2019), "Direct finite element method for nonlinear earthquake analysis of concrete dams: Simplification, modeling, and practical application", *Earthq. Eng. Struct. Dyn.*, **48**(7), 818-842. <https://doi.org/10.1002/eqe.3150>.
- Lu, Y., Hajirasouliha, I. and Marshall, A.M. (2016), "Performance-based seismic design of flexible-base multi-storey buildings considering soil-structure interaction", *Eng. Struct.*, **108**, 90-103. <https://doi.org/10.1016/j.engstruct.2015.11.031>.
- Mandal, A. and Maity, D. (2019), "Seismic analysis of dam-foundation-reservoir coupled system using direct coupling method", *Couple. Syst. Mech.*, **8**(5), 393-414. <https://doi.org/10.12989/csm.2019.8.5.393>.
- Mejia-Nava, R.A., Ibrahimbegovic, A., Dominguez-Ramirez, N. and Flores-Mendez, E. (2021), "Viscoelastic behavior of concrete structures subject to earthquake", *Couple. Syst. Mech.*, **10**(3), 263-280. <https://doi.org/10.12989/csm.2021.10.3.263>.
- Newmark, N.M. and Hall, W.J. (1969), "Seismic design criteria for nuclear reactor facilities", *Proceedings of the 4th World Conference on Earthquake Engineering*, Santiago, Chile.
- Nikolić, M., Do, X.N., Ibrahimbegovic, A. and Nikolić, Ž. (2018), "Crack propagation in dynamics by embedded strong discontinuity approach: Enhanced solid versus discrete lattice model", *Comput. Meth. Appl. Mech. Eng.*, **340**, 480-499. <https://doi.org/10.1016/j.cma.2018.06.012>.
- Plaxis Scientific Manual, Plaxis Reference Manual, Plaxis Material Models Manual (2021), available on <https://communities.bentley.com/products/geotech-analysis/w/plaxis-soilvision-wiki/46137/manuals---plaxis>
- Reza Tabatabaiefar, S.H., Fatahi, B. and Samali, B. (2013), "Seismic behavior of building frames considering dynamic soil-structure interaction", *Int. J. Geomech.*, **13**(4), 409-420. [https://doi.org/10.1061/\(ASCE\)GM.1943-5622.0000231](https://doi.org/10.1061/(ASCE)GM.1943-5622.0000231).
- Robert, E.S. (2009), "Dynamic nonlinear soil-structure interaction", Doctoral Dissertation, Ecole Centrale Paris.
- Santos, J.A. and Correia, A.G. (2001), "Reference threshold shear strain of soil. its application to obtain a unique strain-dependent shear modulus curve for soil", *15th International Conference on Soil Mechanics and Geotechnical Engineering*, Istanbul, Turkey, **1**, 267-270.
- Schanz, T. and Vermeer, P.A. (1998), "Special issue on pre-failure deformation behaviour of geomaterials", *Géotechnique*, **48**, 383-387.
- Schanz, T., Vermeer, P.A. and Bonnier, P.G. (1999), "The hardening-soil model: Formulation and verification", *Beyond 2000 in Computational Geotechnics*, Routledge.
- Seed, H.B. and Lysmer, J. (1978), "Soil-structure interaction analyses by finite elements-State of the art", *Nucl. Eng. Des.*, **46**(2), 349-365. [https://doi.org/10.1016/0029-5493\(78\)90020-1](https://doi.org/10.1016/0029-5493(78)90020-1).
- Tabatabaiefar, H.R. and Massumi, A. (2010), "A simplified method to determine seismic responses of reinforced concrete moment resisting building frames under influence of soil-structure interaction", *Soil Dyn. Earthq. Eng.*, **30**(11), 1259-1267. <https://doi.org/10.1016/j.soildyn.2010.05.008>.
- Zhang, X. and Far, H. (2021), "Effects of dynamic soil-structure interaction on seismic behaviour of high-rise buildings", *Bull. Earthq. Eng.*, **20**(7), 3443-3467. <https://doi.org/10.1007/s10518-021-01176-z>.